

Mechanical behavior and failure modes of aluminum/bamboo sandwich plates under quasi-static loading

G. X. SUI

Department of Mechanical Engineering, Hong Kong University of Science and Technology, Clear Water Bay, Kowloon, Hong Kong, People's Republic of China; Institute of Metal Research, Chinese Academy of Sciences, 72 Wenhua Road, Shenyang 110015, People's Republic of China

T. X. YU, J. K. KIM

Department of Mechanical Engineering, Hong Kong University of Science and Technology, Clear Water Bay, Kowloon, Hong Kong, People's Republic of China
E-mail: metxyu@ust.hk

B. L. ZHOU

Institute of Metal Research, Chinese Academy of Sciences, 72 Wenhua Road, Shenyang 110015, People's Republic of China

Experimental investigations have been made on the quasi-static mechanical behavior and failure modes of aluminum/bamboo sandwich plates. Thermosetting epoxy resin and thermoplastic Polybond resin were used to bond the aluminum sheets and the bamboo. Tensile, compressive and flexural properties were evaluated. The effects of bond conditions on the mechanical behavior and failure modes were examined. The thermoplastic Polybond resin resulted in a stronger interface bond than the thermosetting epoxy resin. The improvement of the interface bond led to significant increases in compressive and flexural properties. The tensile properties were found to be insensitive to the interface bond. The dominant failure mechanisms affected by the interface bond dictated the mechanical properties of the sandwich plates in individual loading conditions. © 2000 Kluwer Academic Publishers

1. Introduction

During the past decades, bamboo has become an attractive object of study not only for botanists, but also for material scientists, and engineers and designers alike. Regarding it as a natural composite the microstructures and the mechanical properties of bamboo were extensively studied [1–4]. The microstructures of bamboo, such as the distribution and fine structure of bamboo fibers, were mimicked to design engineering composite materials [5, 6]. The bamboo fibers were also extracted from raw bamboo and were incorporated into a polymeric resin to make bamboo fiber/polymer matrix composites [7–9]. Furthermore, a technique was developed to reform the bamboo through the treatment involving softening, compression and fixture processes [10]. After the reforming treatment, the cross-sectional shape of bamboo was changed from the natural circular form into a rectangular form, with its properties becoming denser and stronger than the previous form of natural bamboo. The reformed bamboo plates are more convenient to handle for engineering applications than the natural bamboo, though the natural bamboo possesses an optimal structure [5]. The reformed bamboo plates

were bonded with aluminum sheets, generating aluminum/bamboo sandwich plates [11]. A preliminary study of these sandwich materials has shown that they possess extraordinary mechanical properties. In many practical applications, a sandwich design approach is most efficient in enhancing stiffness and strength, particularly in bending. The role of faces is to provide the required bending and in-plane shear stiffness and to carry the axial and bending stresses, whereas the core is to carry the shear stresses between the faces [12]. By virtue of their low cost for materials and production, and their high strength/weight ratio, the aluminum/bamboo sandwich plates have good potential applications, such as air cargo containers, tailor boxes, mobile homes, etc.

In the present research work, experimental studies were made on large-size aluminum/bamboo sandwich plates. Two different types of adhesive were used to bond the aluminum sheets and the reformed bamboo: a thermosetting epoxy resin and a thermoplastic Polybond resin. The tensile, compressive and flexural properties are evaluated. Special emphasis is placed on the study of the effects of the interface bond on the mechanical behavior and failure modes.

2. Experimental

2.1. Materials

The raw materials used for manufacturing aluminum/bamboo sandwich plates comprise: (i) LY12CZ aluminum alloy sheets (similar to Al-2024T6) with a thickness of 0.3 mm; (ii) reformed bamboo slabs with a width of about 50 mm and a thickness of about 5–6 mm; (iii) bisphenol-A epoxy resin 6101 hardened with 651 polyimide resin (supplied by Shenyang Resin Factory, China); and (iv) a chemically modified high density polyethylene (Polybond 3009 supplied by Unirol Chemical Company, Inc., USA).

Aluminum/bamboo sandwich plates were bonded using the thermosetting epoxy resin and the thermoplastic Polybond in two lay-up configurations, unidirectional (Al/0°/0°/Al) and cross-ply (Al/0°/90°/Al), as shown schematically in Fig. 1. The epoxy-bonded and the Polybond-bonded aluminum/bamboo sandwich plates (designated as EAB and PAB, respectively) were manufactured in planar sizes of 640 mm × 500 mm and 300 mm × 300 mm, respectively. The final thickness of the plates ranged 11–14 mm due to the variations in thickness of the bamboo slabs. Further details of sandwich fabrication procedure can be found elsewhere [11, 13].

2.2. Tests and specimen preparations

Tensile, compressive and three-point bending tests were carried out to evaluate the mechanical properties of the aluminum/bamboo sandwich plates. The specimens were prepared in three groups according to the bamboo fiber orientation: longitudinal direction of the unidirectional plates (designated as L); transverse direction of the unidirectional plates (T); and one of two main directions of the cross-ply plates (C). All specimens were cut from the plates described above and then machined to the required shapes, as shown in Fig. 2.

Tensile tests were performed on a MTS810 universal testing machine with a maximum load capacity of 100 kN, while compressive tests were performed on a MTS815 rock mechanics testing machine with a maximum load capacity of 1000 kN. The load was applied at a constant loading rate of 0.3 mm/min at ambient temperature. The average stress was calculated from the load divided by the cross-sectional area within the uniform portion of the specimen without due regard to the difference in component material properties. The average strain was measured using an extensometer with a gauge length of 25 mm which was attached to the middle of the uniform portion of the specimen. Therefore, the stress-strain curves shown in the following represent those of sandwich as a whole. For the cross-ply specimens, the extensometer was

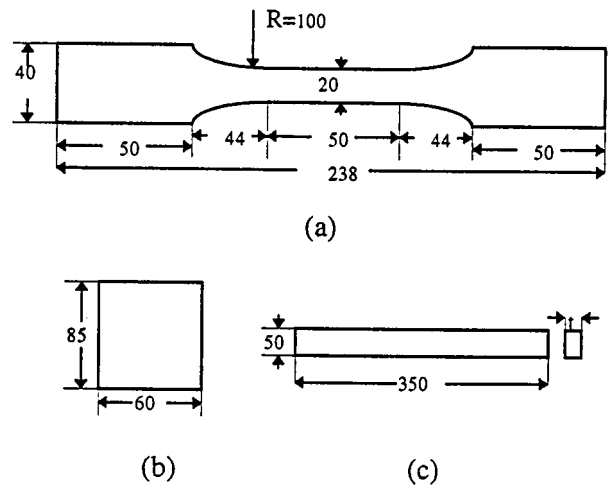


Figure 2 Specimen dimensions (in mm) for (a) tensile; (b) compressive; and (c) three-point bending tests.

attached to the side with bamboo fibers parallel to the loading axis. Data acquisition was carried out using a personal computer interfaced with the testing machine.

Three-point bending tests were performed on a MTS810 universal testing machine with a maximum load capacity of 100 kN. The radii of the fixture supporters and the indenter head were all 5 mm. The span was set at 300 mm for the EAB specimens and 290 mm for the PAB specimens because of the limitation of the material length. The minor difference in the span did not affect the comparability of the flexural properties of the plates. The cross-ply specimens were loaded with the longitudinal bamboo layer on the tension side. The load was applied at a rate of 1.5 mm/min. The central deflection was taken from the LVDT of the testing machine. The flexural strengths and moduli were calculated from the load-deflection curves according to the beam bending theory.

3. Results and discussions

3.1. Tensile behavior and tensile failure modes

The typical average tensile stress-strain curves shown for the EAB and PAB plates in Fig. 3a and b suggest that the unidirectional plates behaved elastically until they failed catastrophically without any presage. The EAB specimens always failed by fracture or splitting of bamboo, or by fracture of one bamboo layer followed by delamination between bamboo layers. The aluminum sheets seldom fractured when the bamboo failed, and became debonded from the bamboo core followed by being buckled during unloading the specimens, as shown in Fig. 4a. In sharp contrast, the PAB specimens

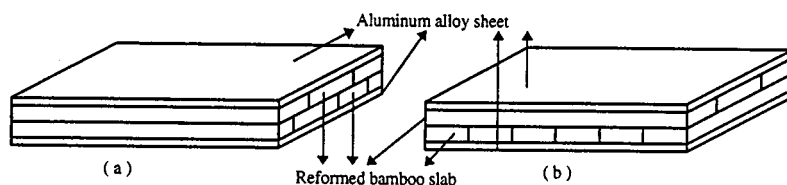
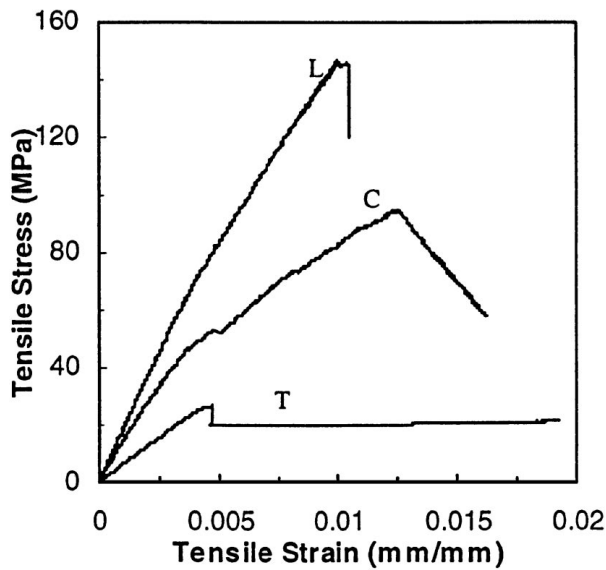
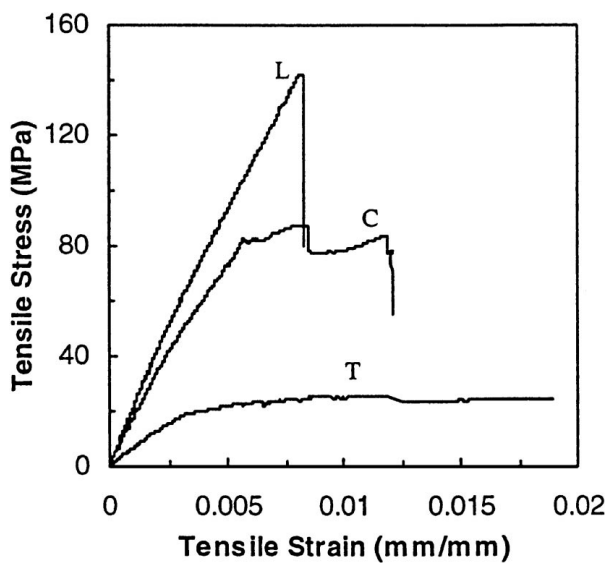


Figure 1 Schematic illustration of aluminium/bamboo sandwich plates: (a) unidirectional (Al/0/0/Al); (b) cross-ply (Al/0/90/Al).



(a)



(b)

Figure 3 Tensile stress-strain curves of (a) EAB and (b) PAB plates tested in the longitudinal (L) direction of unidirectional plates; the transverse (T) direction of unidirectional plates; and one of the main axes of cross-ply plates (C).

failed mainly by fracture and splitting of the bamboo core, accompanied by fracture of aluminum sheets. Neither delamination between the bamboo layers nor debonding of the aluminum sheets from the bamboo core was observed during and after the test, as shown in Fig. 5a. The peel test and shear test showed that Poly-bond provided a stronger interface bond between aluminum and bamboo than the epoxy resin [13]. The high bond strength of the interfaces in PAB plates restrained interfacial debonding and shear failure between aluminum and bamboo. Thus, the deformation of the aluminum sheet was concentrated on the site where the bamboo cracking occurred, and consequently caused the complete fracture of bamboo core along with the aluminum sheets.

The unidirectional plates sustained much lower stress level when loaded in the transverse direction than in the longitudinal direction (Fig. 3). The failure of the plates always initiated by cracking at the edge joints between bamboo slabs, or by cracking along the bamboo fibres (Figs 4b and 5b).

The cross-ply plates displayed an average stress level between those for the L and T groups (Fig. 3). It was observed that cracks always initiated at the edge joints between bamboo slabs on the trans-ply layer, or at the microcracks in bamboo arising from the bamboo reforming process. Further propagation of cracks usually caused debonding of aluminum sheets and splitting of the longitudinal bamboo layer in the EAB plates (Fig. 4c). As for the PAB plates, the cracks on the trans-ply layer, once initiated, propagated quickly through to the longitudinal layer and finally caused the failure of the specimen by complete fracture of bamboo core along with the aluminum sheet, or fracture of the aluminum sheet along with bamboo splitting. No debonding between aluminum and bamboo was observed after unloading the specimens (Fig. 5c).

3.2. Compressive behavior and compressive failure modes

The typical average compressive stress-strain curves for the EAB and PAB plates are shown in Figs 6 and 7,

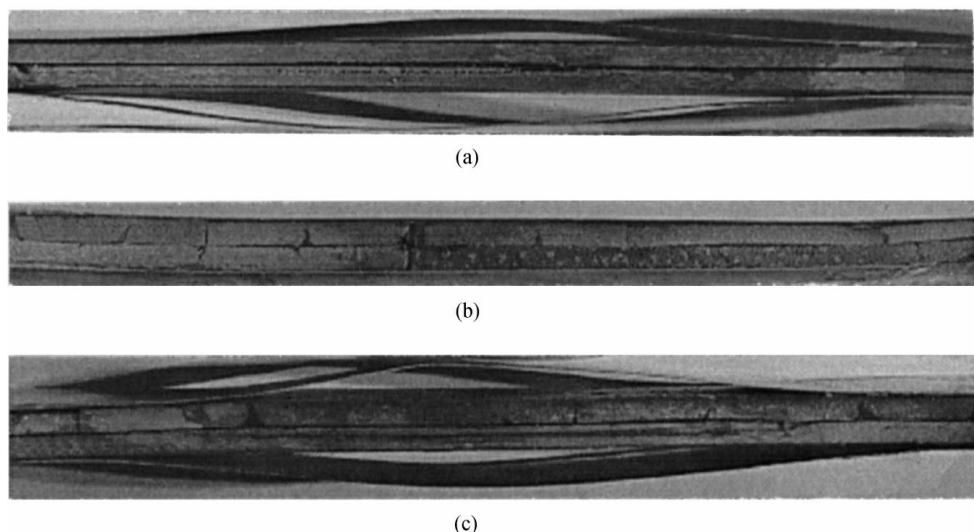


Figure 4 Photographs of failed EAB tensile test specimens: (a) L, (b) T and (c) C orientations.

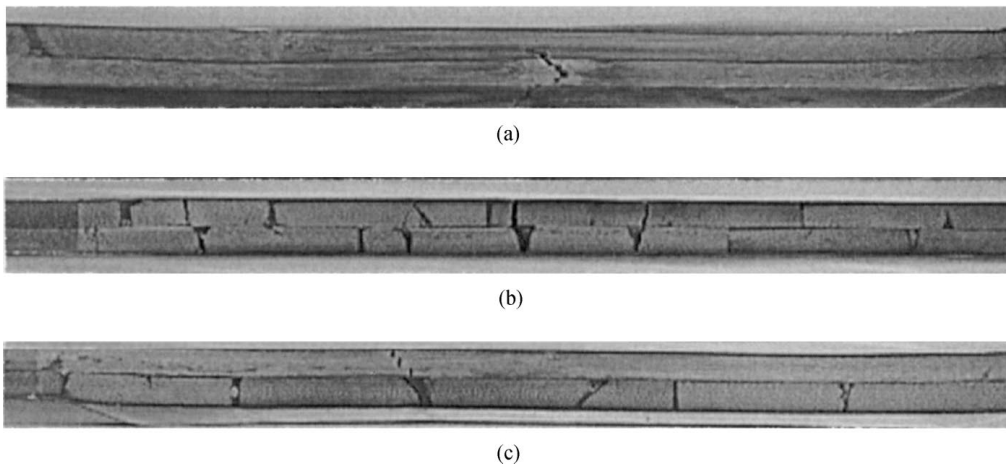
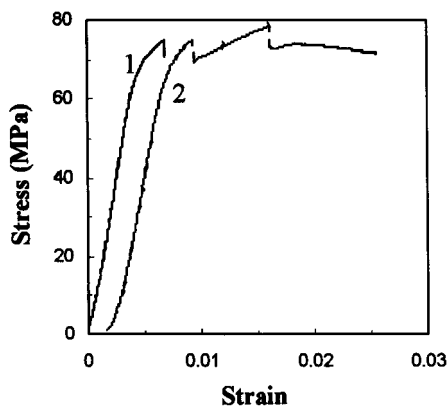
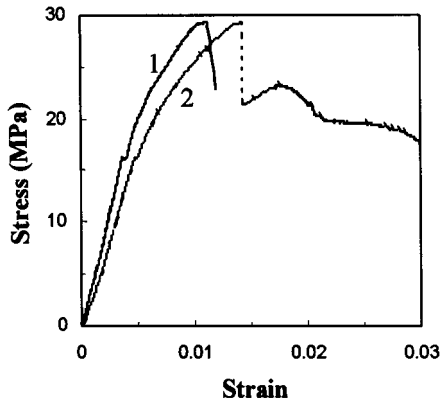


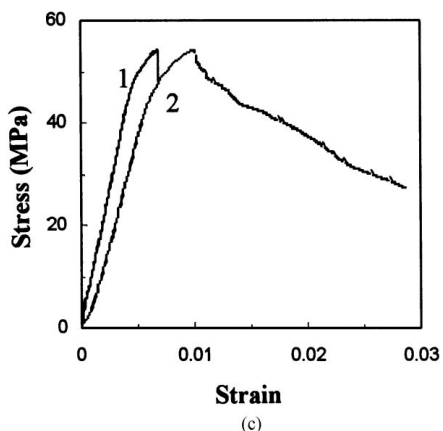
Figure 5 Photographs of failed PAB tensile test specimens: (a) L, (b) T and (c) C orientations.



(a)

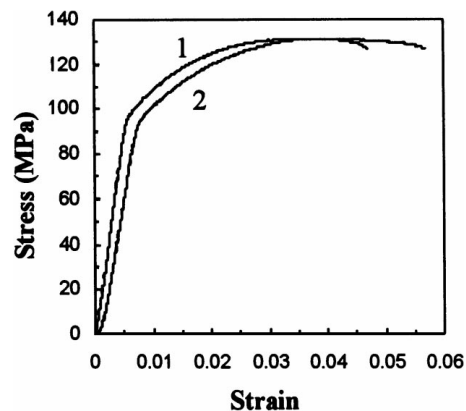


(b)

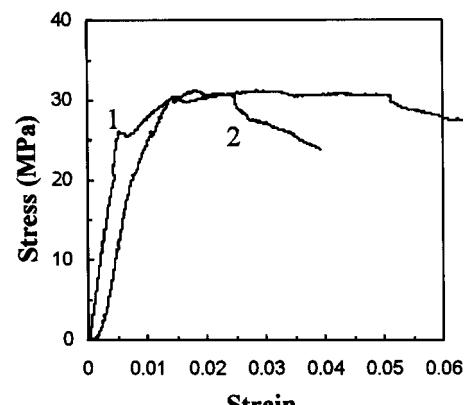


(c)

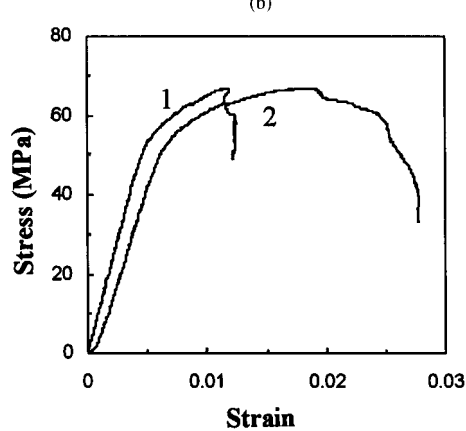
Figure 6 Compressive stress-strain curves of EAB plates in (a) L, (b) T and (c) C orientations. 1-strains measured using extensometers; 2-strains taken from the crosshead displacement records.



(a)



(b)



(c)

Figure 7 Compressive stress-strain curves of PAB plates in (a) L, (b) T and (c) C orientations. Symbols 1 and 2 as in Fig. 6.

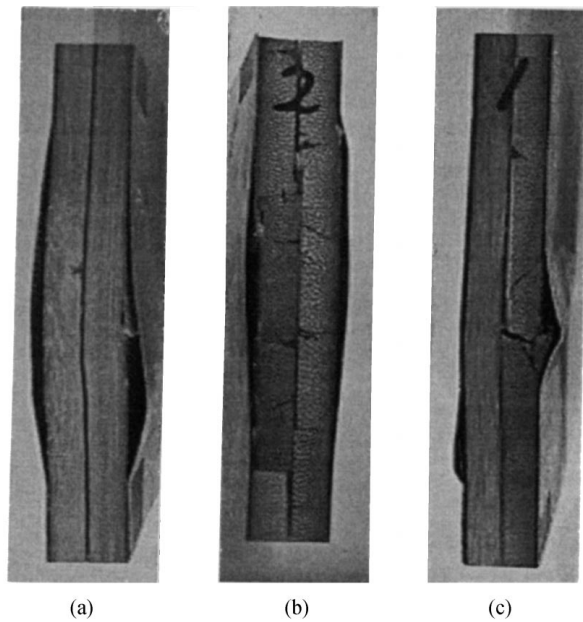


Figure 8 Photographs of failed EAB compressive test specimens: (a) L, (b) T and (c) C orientations.

respectively. Because it became difficult to measure accurately the compressive strain using an extensometer at high strains, the ratio of crosshead displacement to the height of the specimens was also used as strain in Figs 6 and 7. In the longitudinal direction, the unidirectional PAB plates displayed a higher stress level for a given strain than the EAB plates. The failure of the EAB plates was triggered always by debonding and buckling of aluminum sheets. Further deformation led to complete debonding of aluminum sheets and global buckling or kink band formation of the bamboo core (Fig. 8a). No debonding along the interfaces of aluminum/bamboo or bamboo/bamboo was found during the deformation process. Finally, the PAB plates failed by global buckling or shear kinking of the plates (Fig. 9a).



Figure 9 Photographs of failed PAB compressive test specimens: (a) L, (b) T and (c) C orientations.

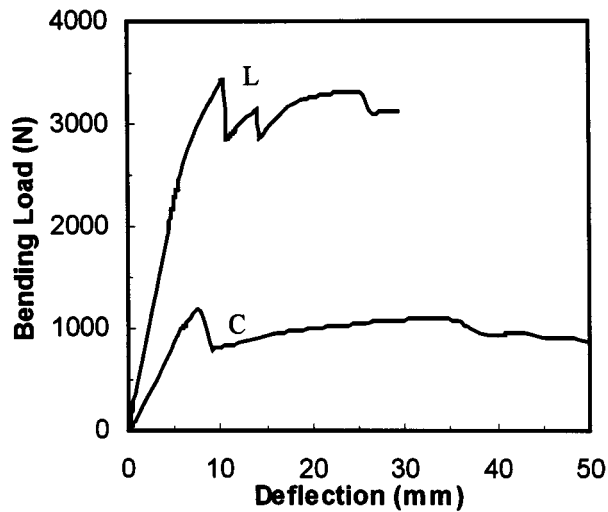
When loaded in the transverse direction, the unidirectional plates displayed a much lower stress level than in the longitudinal direction. The PAB plates showed a little higher stress level than the EAB plates (Figs 6b and 7b). Both plates failed by wrinkling of the aluminum sheets triggered by cracking of the edge joints between bamboo slabs. For the EAB plates, further deformation caused complete debonding and global buckling of aluminum sheets due to the weak interface bond between aluminum and bamboo (Fig. 8b). As for the PAB plates, further deformation led to the developments of wrinkling zones of the aluminum sheets and debonding zones between aluminum and bamboo, while the debonding zones were much smaller than those in the EAB plates (Fig. 9b).

The cross-ply plates deformed under a stress level between those of the L and T groups. The cross-ply PAB plates sustained a higher stress level than the EAB plates, as shown in Figs 6c and 7c. Both plates failed by wrinkling of the aluminum sheets which was triggered by cracking of the edge joints between the trans-ply bamboo layer. Further deformation caused debonding and buckling of aluminum sheets associated with buckling or shear kinking of the bamboo core in the EAB plates (Fig. 8c). Further deformation of the PAB plates, always led to the development of wrinkling zones, accompanied by a local debonding of the aluminum sheet on the side of the trans-ply bamboo layer. No debonding of aluminum sheet was found on the side of longitudinal bamboo layer (Fig. 9c).

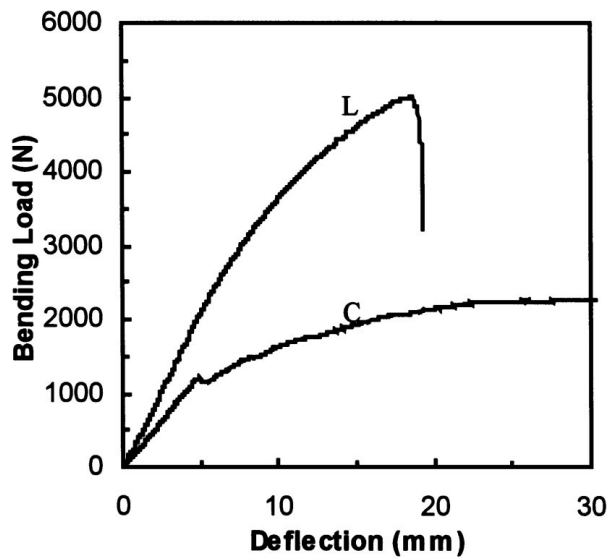
3.3. Flexural behavior and flexural failure modes

The typical three-point bending load-deflection curves are shown in Fig. 10. The EAB plates always failed by debonding and buckling of the upper aluminum sheet, accompanied by sudden load drops as indicated by stick-slips in Fig. 10a. For the L group specimens, the debonding zone developed on both sides of the indenter head, leading to complete debonding of the upper aluminum sheet with further increase of deflection. Meanwhile, the bamboo core deformed plastically at a high deflection (Fig. 11a). For the C group specimens, the increase of the deflection led to the development of the debonding zone of the upper aluminum sheet, accompanied by the fracture of the upper bamboo layer and delamination at the bamboo/bamboo interface (Fig. 11b).

The L group PAB plates failed always by fracture of the lower aluminum sheet as well as the bamboo core (Fig. 12a). No debonding of the upper aluminum sheet was found, due to the high bond strength of the aluminum/bamboo interface. For the C group specimens, the failure always started by cracking at the edge joints of the bamboo slabs on the upper bamboo layer, which further led to formation of a series of wrinkles in the upper aluminum sheet. The material yielded gradually with the development of the wrinkling zones. No fracture was found in the lower bamboo layer and the lower aluminum sheet (Fig. 12b).



(a)



(b)

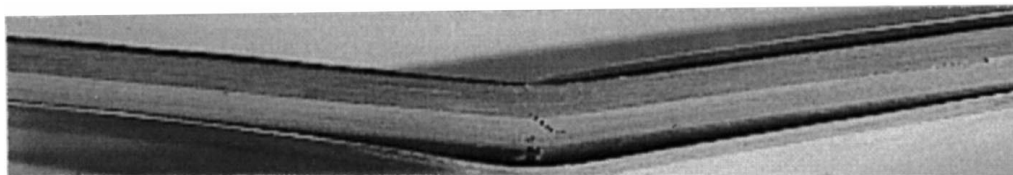
Figure 10 Three point bending load-deflection curves for (a) EAB and (b) PAB plates tested in the longitudinal (L) direction of unidirectional plates; and one of the main axes of cross-ply plates (C).

3.4. Bond conditions, failure modes and mechanical properties

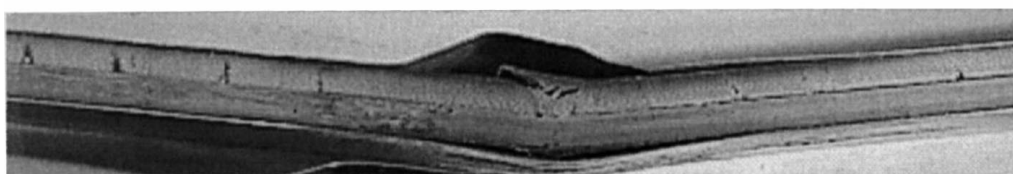
As described above, the aluminum/bamboo sandwich plates showed different failure modes under different

loading conditions. The dominant failure modes under tension, compression and three-point bending are summarized in Table I. Since the PAB plates had a higher bond strength at the aluminum-bamboo interface than the EAB plates, these two plates showed different failure modes, especially when loaded in compression and three-point bending where the material behavior becomes sensitive to the interface bond quality. The changes in the failure mode brought the changes in the mechanical properties of the plates. The major mechanical properties of the aluminum/bamboo sandwich plates are summarized in Table II. The bond strength at the aluminum-bamboo interface was not a critical factor in tension. The improvement in the bond quality did not change the dominant tensile failure mode. Therefore, both the PAB and EAB plates showed little difference in their tensile properties. As shown in Table II, the tensile strengths and the tensile moduli of the PAB and EAB plates with L, T and C orientations displayed only marginal differences.

It was also noted that the L group PAB plates had a larger increase in the compressive properties than the EAB plates, due to the change of the dominant failure modes from interfacial debonding of the aluminum sheet at a lower stress level to kinking or global buckling at a higher stress level. The improvements in compressive properties in T and C group specimens were only marginal within the data scattering range, because of the similar dominant failure modes. However, the flexural properties were most sensitive to the interface bond quality. The debonding of the upper face sheet was always the dominant failure mode for structures without a strongly bonded interface. When the bond conditions were improved significantly, the dominant failure mode shifted to one with a higher stress level. As shown in Table I, once the interface bond became stronger in the L group specimens, the dominant failure mode changed to fracture of the lower aluminum sheet and the bamboo core. In the C group specimens, the edge joints between the upper bamboo slabs became the weakest points after the aluminum/bamboo interface bond was improved. The shifts of the dominant failure modes from lower stress levels to higher ones resulted in remarkable increases in the flexural properties, as shown in Table II.



(a)



(b)

Figure 11 Photographs of failed EAB three point bending test specimens: (a) L and (b) C orientations.

TABLE I Dominant failure modes of aluminum/bamboo sandwiched structures under tension, compression and three-point bending

	EAB			PAB		
	L	T	C	L	T	C
Tension	Fracture of bamboo	Cracking of edge joints of bamboo slabs or cracking of bamboo slabs along grains	Cracking on the trans-ply bamboo layer	Fracture of bamboo along with aluminum fracture	Cracking of edge joints of bamboo slabs or cracking of bamboo slabs along grains	Cracking on the trans-ply bamboo layer
Compression	Debonding of aluminum sheet	Cracking at edge joints and debonding of aluminum sheet	Cracking at edge joints on the trans-ply bamboo layer and debonding of aluminum	Kinking or global buckling	Cracking at edge joints and wrinkling of aluminum sheet	Cracking at edge joints on the trans-ply bamboo layer and wrinkling of aluminum sheet
Three-point bending	Debonding and buckling of the upper aluminum sheet	—	Debonding and buckling of the upper aluminum sheet	Fracture of the lower aluminum sheet associated with the bamboo core	—	Cracking at the edge joints of upper bamboo slabs and the local wrinkling of the upper aluminum sheet

EAB: Epoxy-bonded aluminum/bamboo sandwiched plates; PAB: Polybond-bonded aluminum/bamboo sandwiched plates; L: Longitudinal direction of the unidirectional plates; T: Transverse direction of the unidirectional plates; C: One of two main directions of the cross-ply plates.

TABLE II Major mechanical properties of aluminum/bamboo sandwich plates

	EAB			PAB		
	L	T	C	L	T	C
Tensile strength, MPa	117 ± 24	24 ± 2	87 ± 9	112 ± 20	25 ± 1	78 ± 15
Tensile modulus, GPa	17 ± 1	5.9 ± 0.7	12 ± 1	18 ± 2	5.6 ± 0.4	11.3 ± 0.6
Compressive strength, MPa	71 ± 6	28 ± 3	53 ± 2	119 ± 9	31.9 ± 0.6	62 ± 4
Compressive modulus, GPa	14 ± 1	6 ± 2	11 ± 1	17 ± 1	4.9 ± 0.2	11.0 ± 0.7
Flexural strength, MPa	160 ± 6	—	71 ± 12	265 ± 23	—	116 ± 4
Flexural modulus, GPa	22 ± 1	—	15.4 ± 0.9	27 ± 1	—	14.5 ± 0.3

EAB: Epoxy-bonded aluminum/bamboo sandwiched plates; PAB: Polybond-bonded aluminum/bamboo sandwiched plates; L: Longitudinal direction of the unidirectional plates; T: Transverse direction of the unidirectional plates; C: One of two main directions of the cross-ply plates.

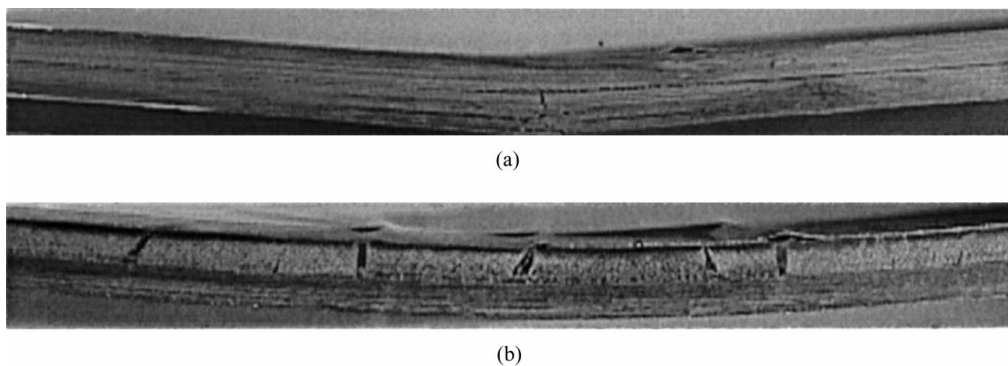


Figure 12 Photographs of failed PAB three point bending test specimens: (a) L and (b) C orientations.

Special mention should be made of the unbalanced cross-ply plates that were used in the tests. Such a configuration would cause bending effects when loaded in tension, which may affect the failure modes of the specimens. In the present case, the coupling effect was noticed. While, it did not cause large changes in failure mode, it appeared to promote, to a certain extent, delamination between bamboo layers.

4. Conclusions

The mechanical properties of aluminum/bamboo sandwich plates have been evaluated under tension, compression and three-point bending. The PAB plates showed superior properties to the EAB plates, due to the stronger aluminum-bamboo interface bond strength. The interface bond quality had a predominant effect on failure mode of the sandwich plates, especially when

subjected to compression and bending. The shifts of the dominant failure modes due to the improvement of the aluminum-bamboo interface bond strength resulted in the enhancement of the mechanical properties of the sandwich plates.

Acknowledgements

The financial support from the Research Infrastructure Grant (RI95/96.EG05) of HKUST is gratefully acknowledged. G.X.S. was a Visiting Scholar from the Institute of Metal Research, Chinese Academy of Sciences (IMRCAS) to the Hong Kong University of Science and Technology (HKUST) when this work was performed. A part of the paper was presented at the Third International Conference on Fracture and Strength of Solids held in December 1997, Hong Kong.

References

1. D. FENGEL and X. SHAO, *Wood Sci Technol.* **18** (1984) 103.
2. N. N. WAI, H. NANKO and K. MURAKAMI, *ibid.* **19** (1985) 211.

3. S. CHUMA, M. HIROHASHI, T. OHGAMA and Y. KASAHARA, *J. Soci. of Mater Sci.* **40**(448) (1991) 21.
4. S. AMADA and R. S. LAKES, *J. Mater Sci.* **32**(10) (1997) 2693.
5. S. H. LI, S. Y. FU, Q. Y. ZENG, X. P. ZHAO and B. L. ZHOU, *Biomimetics*, **2**(1) (1994) 15.
6. S. H. LI, Q. Y. ZENG, Y. L. XIAO, S. Y. FU and B. L. ZHOU, *Mater Sci. & Enginr. C* **C3**(2) (1995) 125.
7. S. JAIN, R. KUMAR and U. C. JINDAL, *J. Mater Sci.* **27**(17) (1992) 4598.
8. S. JAIN, U. C. JINDAL and R. KUMAR, *J. Mater Sci. Lett.* **12**(8) (1993) 558.
9. F. G. SHIN, X. J. XIAN, W. P. ZHENG and M. W. YIPP, *J. Mater Sci.* **24**(10) (1989) 3483.
10. Q. Y. ZENG, S. H. LI, X. R. BAO and B. L. ZHOU, *Scientia Silvae Sinicae* **30** (1994) 253.
11. S. H. LI, S. Y. FU, B. L. ZHOU, Q. Y. ZENG and X. R. BAO, *J. Mater Sci.* **29** (1994) 5990.
12. J. K. KIM and T. X. YU, *J. Mater. Proc. Technol.* **63** (1997) 33.
13. B. H. GUO and X. J. HUANG, Technical Report (RI95/96.EG05-R02), HKUST 1997.

Received 17 April 1998

and accepted 8 April 1999